Electrospun Nanofibers for Regenerative Medicine**

Wenying Liu,
Department of Energy, Environmental and Chemical Engineering, Washington University in St. Louis, St. Louis, MO 63130 (USA)

Prof. Stavros Thomopoulos, and
Department of Orthopaedic Surgery, Washington University School of Medicine, St. Louis, MO 63110 (USA). Department of Biomedical Engineering, Washington University in St. Louis, St. Louis, MO 63130 (USA)

Prof. Younan Xia
Department of Biomedical Engineering, Washington University in St. Louis, St. Louis, MO 63130 (USA)

Younan Xia: xia@biomed.wustl.edu

Abstract

This article reviews recent progress in applying electrospun nanofibers to the emerging field of regenerative medicine. We begin with a brief introduction to electrospinning and nanofibers, with a focus on issues related to the selection of materials, incorporation of bioactive molecules, degradation characteristics, control of mechanical properties, and facilitation of cell infiltration. We then discuss a number of approaches to fabrication of scaffolds from electrospun nanofibers, including techniques for controlling the alignment of nanofibers and for producing scaffolds with complex architectures. We also highlight applications of the nanofiber-based scaffolds in four areas of regenerative medicine that involve nerves, dural tissues, tendons, and the tendon-to-bone insertion site. We conclude this review with perspectives on challenges and future directions for design, fabrication, and utilization of scaffolds based on electrospun nanofibers.

1. Introduction

Many of the tissues in the human body do not have the capacity to regenerate, so damage to these tissues is irreversible.[1] In addition to the poor ability to heal, injuries to tissues such as nerve, tendon, cartilage, and myocardium also result in significant pain and disability. Even with surgical intervention, return of function is often limited and the healing response is scar-mediated rather than regenerative.[2] Patients suffering from organ trauma, disease, or congenital abnormality must rely on organ transplantation to regain function. In spite of its enormous success clinically, this approach is plagued by post-surgical immune reactions and a severe limitation in the number of available donors, leaving thousands of patients on waiting lists.[3] In the United States, 18 people die each day before a suitable organ donor is found.[4] To address these and other issues related to tissue damage and organ transplantation, regenerative medicine has emerged as an interdisciplinary research field that incorporates biology, materials science, and engineering to develop functional substitutes that are safe and readily available for patients with damaged tissues or organs. In

regenerative medicine, elements of scaffold design, cellular control, and signaling are integrated to enhance healing or replace an injured tissue or organ.[5]

One of the major challenges in regenerative medicine is to design and fabricate a suitable scaffold. In order to achieve the desirable functionality of the tissue or organ to be replaced, the scaffold needs to be carefully engineered to elicit specific responses from local cells and organ systems.[6] In one approach, a donor organ is decellularized and the remaining extracellular matrix (ECM) is used as a scaffold. [7] The scaffold is then seeded with patient-specific cells to create a functional substitute for implantation. Although this new strategy can mitigate the immune response commonly seen with the conventional transplantation approaches by using patient-specific cells, the availability of organs that can be used for decellularization remains a stringent limitation.[1] This limitation has inspired biomedical engineers to construct tissues and organs in the laboratory using synthetically derived scaffolds. To this end, cells are cultured on different scaffolds and then a whole organ is assembled from multiple cell-scaffold constructs.

Historically, cells were grown and studied as monolayers on tissue culture plates. In recent years, advances in biomaterial synthesis and microfabrication have made it possible to pattern cells into complex, three-dimensional structures by using appropriate scaffolds as the templates.[8] With an ever-growing understanding of the intricate interactions between cells and their microenvironments in tissues, more attention is now given to the fabrication of scaffolds capable of recapitulating key features of the ECM that control the migration, proliferation, and differentiation of cells.[9] The ECM is often composed of interwoven protein fibers such as fibrillar collagen and elastin, with diameters ranging from tens to hundreds of nanometers. This matrix also contains nanoscale adhesion proteins that serve as specific binding sites for cell adhesion.[10] Signaling to cells from the ECM occurs by direct interactions between ligands on the ECM and cell receptors, the sequestration of growth factors by the ECM, spatial cues, and mechanical force transduction.[10] As such, the microenvironment provided by the ECM can control the behavior and fate of a cell.[11] Many techniques have been developed for fabricating fibrous scaffolds to be used as ECM substitutes;[12] electrospinning has recently emerged as one of the most successful techniques, owning to its ability to generate fibers similar to the fibrous structures of native ECM.

Electrospinning is a remarkably simple, robust, and versatile technique capable of generating fibers with diameters down to the nanoscale.[13] A non-woven mat of electrospun nanofibers possesses high porosity and spatial interconnectivity well-suited for nutrient and waste transport and cell communication.[14] A scaffold based on electrospun nanofibers also has a large specific surface area for loading of bioactive molecules to facilitate efficient and selective cellular responses. Electrospinning has been applied to more than 100 different types of polymers.[13] Naturally occurring matrix proteins including collagen, elastin, and fibrinogen and synthetic polymers such as poly(ε-caprolactone) (PCL) and poly(lactic-co-glycolic) acid (PLGA) can all be prepared as nanofibers by electrospinning.[15] Since different tissues have distinct criteria for scaffold functionality, having a wide range of materials to choose from allows one to articulate the compositions and other properties of electrospun nanofibers to meet different demands. In addition, many tissues, including the sciatic nerve,[16] heart,[17] tendon,[18] and blood vessel,[19] have unique anisotropic structures and architectures (Fig. 1) that cannot be recapitulated by scaffolds fabricated using conventional methods. Electrospinning, in contrast, can be easily used to generate assemblies of aligned nanofibers to mimic the anisotropy of these tissues. To this end, scaffolds based on electrospun nanofibers with various alignments have shown superior capacity in shaping cell morphology,[20] guiding cell migration,[21] and affecting cell differentiation[22] when compared to other types of scaffolds both *in vitro* and *in vivo*.

The aim of this article is to provide a review of recent work using electrospun nanofibers as scaffolds for regenerative medicine. We emphasize how the alignment of electrospun nanofibers can be controlled to present the right structural cues for the manipulation of cell attachment, proliferation, and migration *in vitro* and *in vivo*. We also highlight the applications of nanofiber-based scaffolds in four different areas that involve nerves, dural tissues, tendons, and the tendon-to-bone insertion site.

2. Electrospinning of nanofibers

2.1 Setup and principle

Four major components are required for electrospinning (Fig. 2, center):[13] a spinneret (e.g., a hypodermic needle with blunt-tip), a syringe pump for ejecting the polymer solution at a controlled rate, a direct current (DC) power supply up to 30 kV, and a grounded collector (e.g., a piece of aluminum foil). When the polymer solution emerges from a spinneret, it initially forms a droplet due to the confinement of surface tension. If a high voltage is applied to the spinneret, charges of the same sign will be built on the surface of the droplet. Once the repulsion among the charges is sufficiently strong to overcome the surface tension, a Taylor cone will be formed, followed by a liquid jet directed towards the grounded collector. The jet will experience both solvent evaporation and whipping instability before it reaches the collector. As a result of stretching by electrostatic repulsion and whipping, the liquid jet will be continuously reduced in size until it has been solidified or deposited on the collector. By adjusting experimental parameters such as the concentration of polymer solution, the voltage, and the distance between spinneret and collector, fibers with uniform diameters can be routinely produced.

2.2 Materials consideration

Electrospinning has already been successfully applied to generate nanofibers from more than 100 different types of synthetic and natural polymers.[23] Synthetic polymers are relatively less expensive and more convenient to work with than natural polymers. For scaffold fabrication, the most commonly used synthetic polymers include PCL, PLGA, poly(ethylene oxide) (PEO), and poly(L-lactic) acid (PLA). Although these polymers are biocompatible and biodegradable, they may cause significant inflammation and foreign body reaction when implanted *in vivo*.[24] Natural polymers are therefore more desirable to avoid complications from severe immune reaction. The most abundant natural polymers are type I and type III collagens; together they account for almost one third of the proteins in the human body.[13] Nanofibers electrospun from collagens will swell when exposed to the moisture in air and tend to lose their fibrous morphology in a short period of time.[25] Cross-linking is thus required to maintain the fibrous morphology after electrospinning.[26] The toxicity associated with some of the cross-linkers may compromise the usefulness of such nanofibers *in vivo*. Additionally, the mechanical strength of collagen nanofibers are typically very weak.[27] To improve stability and mechanical strength, collagens are often mixed with other polymers and then electrospun into fibers.[28] For example, Boyce and co-workers have demonstrated electrospinning with a blend of collagen and PCL. Tensile testing indicates that even inclusion of PCL at a low concentration of 10% could significantly improve the stability and stiffness of the nanofibers.[29]

2.3 Incorporation of bioactive molecules

Bioactive molecules released from a scaffold at a controlled rate can be used to stimulate the proliferation and differentiation of seeded cells during *in vitro* culture, thereby encouraging tissue regeneration after implantation *in vivo*.[30] Many different types of bioactive molecules have been incorporated into scaffolds of electrospun nanofibers, including growth factors.[31] Growth factors are endogenous proteins capable of binding to cell receptors and

directing cellular activities.[32] The biggest challenge in incorporating a growth factor into a scaffold is how to preserve its bioactivity. Several factors in an electrospinning process can lead to deactivation of a growth factor: the high voltage applied,[33] the high density of charges built on the nanofiber,[34] and the involvement of an organic solvent.[35] The last problem can be potentially solved by adding a hydrophilic component such as PEG or hydroxyapatite (HAp), which can bind to the growth factor and protect it from deactivation by an organic solvent during electrospinning.[36] The acidic degradation products of some synthetic polymers (e.g., PLGA) is another potential source of deactivation for the growth factor. A porogen such as PEG can be added into the scaffold to facilitate the diffusion of degradation products and thereby maintain the local pH.[37] However, this approach is limited by its destructive effect on the integrity of the nanofibers.

Successful delivery also depends on the release profile of bioactive molecules incorporated into the scaffold. There are currently four methods for incorporating bioactive molecules into a scaffold:[38] physical adsorption, covalent attachment, electrospinning with a co-axial spinneret (Fig. 2, top left),[39] and addition of bioactive molecules to the electrospinning solution (Fig. 2, top right).[40] Different methods of incorporation typically result in distinct release profiles. For physical adsorption, growth factors are attached to the scaffold mainly through electrostatic interactions. Although this is the simplest way to incorporate growth factors with relatively high bioactivity, the release is typically rapid. One study reported a burst release during the first 5 days, with complete release within 20 days.[36] The release profiles for scaffolds prepared by electrospinning with a co-axial spinneret or from a solution mixed with bioactive molecules are similar to each other: there is an initial burst release followed by a sustained, first order release.[41] The initial burst release can be attributed to the migration of the growth factors during the drying process, which tends to concentrate a certain fraction of the growth factor molecules near the surface of the fibers. After burst release, the release mode is primarily driven by diffusion and polymer degradation.[42] Jeong and co-workers developed a method to program the release of the bioactive molecules.[40] They first encapsulated the bioactive molecules in cross-linked polymer particles, which were then blended with a polymer solution and electrospun through a single nozzle. The polymer particles must be cross-linked so they were just swollen in the electrospinning solution instead of being dissolved. By adjusting the physical and chemical properties of the particles, programmed release was achieved. For covalent attachment, burst release is avoided since the release is typically controlled by enzymatic cleavage.[43] However, covalent attachment cannot be employed to routinely load electrospun nanofibers with bioactive molecules due to the technical complexity required for fabrication.

2.4 Degradation characteristics

Once implanted in the body, the scaffold should undergo degradation at a rate matching that of tissue regeneration. For individual nanofibers, the degradation profile is mainly determined by the polymer itself as hydrolysis of the polymer backbone is believed to be the prevailing mechanism.[44] Most of the synthetic polymers are semi-crystalline, implying that their chains fold into crystalline regions in addition to amorphous regions.[45] In the absence of an enzyme, water penetrates the surface of a nanofiber and preferentially attacks the amorphous regions first, converting the long polymer chains into shorter and eventually water-soluble species. Since the crystalline regions are still intact, the nanofiber does not fall apart. As hydrolysis continues, the nanofiber eventually starts to disintegrate and disappear. In the presence of an enzyme, the nanofiber can be digested by the enzyme, resulting in a rapid loss of mass.[46]

When assembled into a scaffold, the structure of the scaffold also plays a very important role in determining the degradation profile of nanofibers. When compared with a thin film cast from the same polymer, a scaffold made of electrospun nanofibers has a higher porosity and

therefore the degradation product will be able to diffuse away more quickly. Otherwise, the accumulation of acidic degradation products will act as a catalyst to make the degradation process faster. As a result, a scaffold based on electrospun nanofibers would require a longer time to degrade than a bulk film of the same mass due to the difference in porosity. [47] Some researchers have also attributed the slow degradation rates of nanofiber scaffolds to the increase in chain orientation and thus higher crystallinity,[48] as the strong electric field involved in an electrospinning process tended to align the polymer chains parallel to the field.[49]

The porosity of a nanofiber-based scaffold is a key factor in controlling the degradation profile. A number of methods have been developed for manipulating the porosity of a nanofiber scaffold, including those based on variation of the size of nanofibers, salt leaching, cryogenic electrospinning, and removal of a sacrificial component. These methods will be discussed in Section 2.6, as cell infiltration is also affected by the porosity.

2.5 Mechanical properties

The mechanical properties of a nanofiber-based scaffold depend on a number of parameters, including the composition, molecular structure, and size of individual nanofibers, as well as the alignment and density of the nanofibers.[50] For example, scaffolds made of PLGA nanofibers can be ten times stiffer than scaffolds made of PCL nanofibers.[51] Ramakrishna and co-workers have found that the rotating speed of a mandrel was a dominant parameter in inducing a highly ordered molecular structure in an electrospun PLLA fiber, which consequently led to higher tensile modulus and strength.[52] Leong and co-workers reported an increase in both strength and stiffness as the fiber diameter was reduced from ~5 μm to ~200 nm.[53] Encapsulation of different drugs may also exert different impacts on the mechanical properties of a single nanofiber. An increase in mechanical strength was reported when 10–20 wt% retinoic acid was encapsulated whereas an opposite trend was observed when 10–20 wt% bovine serum albumin (BSA) was added.[53]

Alignment of nanofibers results in significant stiffening in the direction of alignment and increased scaffold anisotropy.[54] This is an important feature to mimic when engineering anisotropic load-bearing tissues such as tendons, annulus fibrosis, and myocardium. Mauck and co-workers recapitulated the complex tissue organization and mechanical properties of the annulus fibrosus with anisotropic, nanofibrous laminates seeded with mesenchymal stem cells.[55] The scaffolds approached the mechanical properties of native tissues after 10 weeks of culture. Modification of the surface of the fibers with precipitated bioapatite can also lead to dramatic increases in scaffold stiffness.[56]

The mechanical properties of scaffolds can have strong impacts on cell proliferation and stem cell differentiation. Discher and co-workers demonstrated that the commitment of stem cells to a particular phenotype was highly dependent on the stiffness of substrate.[57] The most compliant surfaces were neurogenic while the stiffest matrices were osteogenic. Ingber and co-workers demonstrated that cell phenotypes could be affected by cellular adhesion to the ECM and the mechanical tension in cytoskeleton.[58] In general, rigid substrates tend to promote cell spreading by resisting cell tension.[59] Rigid substrates supporting higher levels of isometric tension in the cell allow spreading and growth of cells such as fibroblasts and endothelial cells. Flexible substrates that cannot withstand stretching will result in retracting, rounding up, and the down regulation of genes associated with proliferation.[60] Controlling the mechanical properties of both bulk and individual nanofibers will help optimize scaffolds for tissue regeneration by recapitulating the properties of the tissue being replaced and by providing the appropriate cues for the seeded cells.

2.6 Cell infiltration

The porosity of a nanofiber scaffold can directly affect the infiltration of cells.[61] Although many research groups have focused on the development of fibers with reduced diameters to increase the specific surface area for loading of bioactive molecules, it has been shown that the scaffolds consisting of thinner fibers tend to have a lower porosity due to a denser packing of the fibers.[62] One technique for increasing the porosity of a scaffold is based on salt leaching. The setup for this technique is identical to that of electrospinning with a co-axial spinneret (Fig. 2, top left). The nanofibers produced using this technique had a core-sheath structure with the polymer as the core and crystals of the salt in the sheath. The high voltage was able to stretch the jet of polymer solution into a nanofiber while the salt crystals were formed and attached to the surface. The salt crystals were then dissolved in water to generate a mat with high porosity, which could facilitate cell infiltration up to 4 mm in depth.[63] Other approaches include selective removal of sacrificial fibers in a scaffold prepared using a dual spinneret system.[64] To this end, Mauck and co-workers co-electrospun PCL and PEO (a water-soluble polymer) from two separate spinnerets to form a dual-polymer scaffold (Fig. 2, bottom left). The PEO fibers were dissolved gradually in the cell culture medium and cells were found to be present throughout the entire scaffold.[64c] Although these two methods could considerably improve cell infiltration, they also led to compromised structural integrity and macroscopic delamination. Recently, Jun and co-workers developed a semi-spherical bowl with small needles randomly distributed on the inner surface to fabricate cotton-ball-like, uncompressed scaffolds of electrospun nanofibers (Fig. 2, bottom right).[65] This type of scaffold has very high porosity and encourages inward cell migration. The major limitation of this type of scaffold is the difficulty of transferring it to other substrates without destroying its hierarchal structure.

Although many efforts have been devoted to increasing the infiltration of cells into a nanofibrous constructs, a robust and transferrable scaffold has yet to be developed and remains a major goal of future work.

3. Controlling the alignment of nanofibers

In many applications, it is desirable to have a scaffold made of aligned nanofibers, as the anisotropy in topography and structure can greatly affect not only the mechanical properties but also cell adhesion, proliferation, and alignment. Aligned fibrous scaffolds may thus be useful in replicating the ECM for a specific tissue type such as tendon, where collagen fibrils are aligned parallel to each other. To this end, Ouyang and co-workers studied human tendon stem/progenitor cells (hTSPCs) cultured on scaffolds made of aligned or random PLLA nanofibers. Tendon-specific genes were up-regulated in hTSPCs cultured on the aligned nanofibers compared to those on the random fibers.[18] Another example is cardiac tissue, where the ventricular myocardium is composed of perpendicularly interwoven collagen stripes. This unique anisotropy in cardiac tissue gives rise to its special directionally dependent electrical and mechanical properties. Entcheva and co-workers showed that primary cardiomyocytes cultured on a scaffold of aligned PLLA nanofibers developed mature contractile machinery (sarcomeres). Excitability of the engineered constructs was confirmed by optical imaging of electrical activity using voltage-sensitive dyes.[17]

Besides mimicking the ECM, the alignment of electrospun nanofibers in a scaffold can also guide the migration and extension of cells. For example, aligned electrospun nanofibers have been used to guide the neuronal growth from neural stem cells (NSCs). Ramakrishna and coworkers have shown that axons of up to $100\,\mu m$ were formed on aligned fibers, which could be attributed to the enhanced contact guidance.[66] We have also demonstrated that electrospun nanofibers with a uniaxial alignment could induce the differentiation of

mouse embryonic stem cells (ESCs) into neural lineages with less possibility of scar tissue formation.[67] The alignment associated with the fibers can also accelerate the rate of wound closure. This is because the alignment confines the migratory route of the cells to a certain direction so that a shorter time will be needed for cells cultured on aligned nanofibers to cover the same area comparing with those cultured on random nanofibers.[68] As a demonstration, we have recently shown that dural fibroblasts could cover the entire scaffold with a radial alignment at a faster speed relative to a scaffold made of random nanofibers.[69]

A number of methods have been developed for controlling the alignment of electrospun nanofibers. These methods can be categorized into three major categories depending on the type of forces involved (Fig. 3): mechanical, electrostatic, and magnetic. These methods are described in the subsequent sections.

3.1 Alignment caused by mechanical forces

In order to align nanofibers using mechanical forces, a metallic rotating mandrel is often used as the collector (Fig. 3A). When the electrospun nanofibers are collected by a rotating mandrel, the rotating speed of the mandrel determines the degree of alignment of the non-woven mat. Bowlin and co-workers showed that random collagen fibers were collected at linear velocity lower than 0.16 m s^{-1}, while significant alignment was observed at linear velocities higher than 1.4 m s^{-1}.[25a] Whereas a higher speed can result in better alignment, a linear velocity higher than 45 m s^{-1} will encourage formation of necks in the nanofibers. At very high rotation speeds, the velocity of the electrospinning jet may be slower than the linear velocity of the mandrel; this may create stress residues and thus necking in the nanofibers. In order to obtain aligned, uniform nanofibers, it is essential to rotate the mandrel at an appropriate and well-controlled speed. [70]

The alignment of nanofibers collected by conventional rotating mandrels can sometimes be affected by the mandrel width, as the two ends of the collector can act as electrodes too and exert electrostatic forces on the fibers, influencing their alignment. Yarin and co-workers modified the design of a drum by replacing it with a tapered, wheel-like disk.[71] A typical disk is significantly thinner than a commonly used mandrel and the fibers are mostly collected on the sharp edge. The authors also simulated the electrostatic field of the rotating disk and revealed that the field strength increased dramatically near the edge of the disk, which in turn forced the charged fibers to continuously wound on the edge.[71] The major drawback of a rotating disc is its small collecting area, which limits its application for experiments where fabrication of large scaffolds is desirable. Another alternative collector is to use a drum made of nonconductive materials as the collector. Fann and co-workers attempted to collect aligned fibers on a plastic mandrel that included a sharp metallic pin in the interior. By moving the position of the pin, aligned fibers were obtained.[72] The major disadvantage of this design is that the thickness of the scaffold is limited. The plastic mandrel cannot quickly dissipate the charges on the deposited fibers, and the accumulated charges thus repel the incoming fibers, preventing further deposition. One approach to reduce the accumulation of residual charges is to use an alternating current (AC) power supply instead of the typical DC source. Tepper and co-workers showed that nanofibers of PEO collected on the rotating mandrel showed greater alignment when using an AC rather than DC power supply. The electrospinning jet from an AC system consists of short segments of alternating polarity, which would neutralize each other, thus minimizing charge accumulation and leading to improved fiber alignment.[73] One has to be extremely cautious whenever an AC power supply is used as it may generate a high current between the spinneret and the collector.

3.2 Alignment caused by electrostatic forces

Since electrostatic charges are distributed along the electrospinning jet, an external electric field can be used to manipulate and control the alignment of nanofibers. We have developed a collector consisting of two pieces of conductive substrates which are separated by a void gap to collect uniaxially aligned nanofibers across the gap (Fig. 3B).[74] Nanofibers descending from the spinneret will experience two types of electrostatic forces. The splitting of electric field with electric field lines pointing towards the two electrodes produces the first force. This force will pull the fiber towards the electrodes and further induce opposite charges on the surfaces of the electrodes when the fiber travels to their vicinity. This gives rise to a second force, which stretches the nanofiber across the gap to render it perpendicular to the edges of the electrodes. These two types of electrostatic forces work together to produce a uniaxially aligned array of nanofibers. If the fibers spanning across the void gap discharge very slowly and repel each other, the extent of alignment will be improved with deposition time.[75]

One of the remarkable features associated with the gap technique is that it is convenient to transfer the aligned fibers onto other solid substrates for further applications. Single fibers collected across the gap can be easily picked up and tested without transferring to other substrates. As single fibers are very sensitive to stress and strain, avoiding transferring the single fibers is highly desirable in mechanical testing assays.[76] In particular, it has been established that uniaxially aligned fibers could be directly deposited on an insulating substrate on which the pair-wise electrodes can be patterned. This variant is commonly used to fabricate multilayered constructs by controlling the scheme or the configuration for applying high voltage.[77] The detailed explanation will be provided in Section 4.1.

In addition to uniaxial alignment, it is sometimes desirable to align the fibers into other patterns. For example, scaffolds made of radially aligned nanofibers may improve wound healing by providing contact guidance for cell migration.[69] In this case, radially aligned nanofibers will encourage cells to migrate from the peripheral healthy tissue towards the central, injured site. Radial alignment can be achieved using a ring collector with a point electrode in the center. In order to ensure that all the fibers pass through the central point electrode, the needle electrode should be slightly higher than its peripheral ring collector (Fig. 3C). Since cells tend to migrate along the fibers, cells seeded around the periphery of a radially aligned scaffold would follow the nanofibers and migrate inward to cover the whole scaffold at a speed faster than if they were seeded on a scaffold made of random nanofibers.[69]

Another useful type of alignment can be found in scaffolds that contain arrays of microwells. These scaffolds can be fabricated using an array of metallic beads as the collector (Fig. 3D).[78] Whereas fibers deposited on the beads were randomly oriented, those deposited across the gaps between adjacent beads were uniaxially aligned. The resultant non-woven mat had concave microwells at the positions corresponding to the beads. The size of the microwells and the distance between adjacent microwells can both be tailored to accommodate different applications. Dorsal root ganglia (DRG) cultured in the microwells extended neurites to adjacent microwells and formed neural networks on the entire scaffold.[78] This type of scaffold containing aligned nanofibers and patterned microwells may be a useful platform for research related to cell-cell communication and cell microarray assays.

3.3 Alignment caused by magnetic forces

Alignment of electrospun nanofibers can also be achieved by applying an external magnetic field (Fig. 3E). Jiang and co-workers demonstrated that magnetized poly(vinyl alcohol)

(PVA) fibers could be stretched into parallel fibers over large areas (more than 5×5 cm^2) using a magnetic field.[79] The polymer solution was magnetized by adding a small amount (less than 0.5 wt%) of magnetic nanoparticles. The solution was electrospun into nanofibers in the presence of a magnetic field generated by two parallel-positioned permanent magnets. The magnetic field stretched the fibers across the gap to form a uniaxially aligned array as they landed onto the magnets. Nanofibers of PVA were also electrospun without magnetic nanoparticles in a magnetic field, and they were randomly distributed without any alignment. The authors concluded that the magnetic field could assist alignment of electrospun nanofibers, but only when electrospinning a magnetizable solution in a magnetic field.[79] Yang and co-workers also demonstrated that by increasing the flow rate of the electrospun jet, the morphology of resultant nanofibers would change from uniaxially aligned to wavy.[80] In this case, both PLGA and poly(vinyl pyrrolidone) (PVP) were electrospun at different flow rates in a magnetic field. At a flow rate of 0.5 mL h^{-1}, the PLGA and PVP fibers were straight and uniaxially aligned, while at a flow rate of 3.0 ml h^{-1}, the fibers became wavy in morphology without losing the overall alignment. The authors also concluded that the generation of aligned polymer fibers (both straight and wavy) by magnetic field-assisted electrospinning was independent of the solution and solvent used and did not require the solution to be magnetically active.[80] Although both research groups obtained well aligned nanofibers, their interpretation of the phenomenon was contradictory to each other. Further efforts are needed to investigate the mechanism of alignment for nanofibers electrospun in a magnetic field.

4. Nanofiber scaffolds with complex architectures

Nonwoven mats of electrospun nanofibers can be further processed into scaffolds with complex architectures such as stacked arrays and tubular conduits. Stacked arrays of electrospun nanofibers are made of multiple layers of fibers that are sequentially deposited on top of one another. The main motivation for developing this type of scaffold is to mimic some natural tissue with respect to its biochemical, structural, and mechanical properties, as well as to enable the formation of multilayered tissues. Tubular conduits made of electrospun nanofibers are usually used for applications in vascular or neural tissue engineering as they resemble the hollow structures of these tissues (see Fig. 1). Here we only focus on the fabrication methods for these scaffolds with complex architectures.

4.1 Stacked arrays of nanofibers

Uniaxially aligned nanofibers can be stacked into multilayered films with a controllable, hierarchically porous structure. When a pair of electrodes separated by a void gap is used as the collector, the uniaxially aligned nanofibers can be sequentially transferred onto a substrate.[75] By rotating the substrate between the deposition of different layers, it is fairly straightforward to obtain a multilayered film with the nanofibers in each layer oriented along a different direction. Alternatively, the void gap can be replaced by a highly insulating substrate such as quartz or polystyrene. By patterning the collector into an array of electrodes on an insulating substrate, the deposition of nanofibers can easily be directed to generate a multilayered film (Fig. 4A). In one study, this was achieved by alternating the scheme for applying the high voltage.[77] The nanofibers in each layer were uniaxially aligned, with their long axes rotated by 60 degrees between adjacent layers (Fig. 4B). We have applied this type of multilayered scaffold to neural tissue engineering and showed that neurites derived from embryonic stem cells (ESCs) followed the pattern of the underlying scaffold, including at the intersection of two perpendicular fibers.[81] Wang and co-workers also developed scaffolds using a layer-by-layer approach.[82] They first deposited a layer of random fibers mat on a grounded electrode, which was immersed in cell culture medium. Cells were then seeded onto the first layer of the scaffold, after which the second layer of fibers was directly electrospun on top of the cells (Fig. 4C). By repeating these two steps,

scaffolds with a multilayered architecture and embedded with cells were constructed. Figure 4D shows the cross-sectional fluorescent image of the cell-fiber construct, with the fibers in green and cell nucleus in blue. A major advantage of this approach is that the composition of the fibers can be easily tailored. Different growth factors or drugs can be encapsulated in different layers, and the topography of each layer can also be altered.

4.2 Conduits assembled from nanofibers

Conduits comprised of random or circumferentially aligned fibers can be readily fabricated by depositing nanofibers on a rotating mandrel.[70b] However, conduits with nanofibers aligned parallel to the long axis of the tube are sometimes more desirable as cells could then be guided to migrate along the tube. To address this issue, Ramakrishna and co-workers developed a method for fabricating a tube consisting of diagonally aligned electrospun fibers through a combination of electrostatic and mechanical forces.[83] A knife-edged auxiliary electrode was charged with a polarity opposite to the spinneret and placed at a 45-angle relative to the long axis of the rotating Teflon tube, creating an electrostatic field that promoted a diagonal alignment for the nanofibers deposited on the collector. By rotating the Teflon tube, they obtained a tubular conduit with uniform thickness and superior mechanical strength. Chang and co-workers also developed an electrostatic method for fabricating multiple, interconnected conduits composed of electrospun fibers (Fig. 4E).[84] In this case, nanofibers were deposited on collectors with different designs or structures. Upon removal of the collectors, nanofiber conduits with desired configurations were obtained. Alternatively, a tubular conduit can also be fabricated by simply rolling up a nonwoven mat of electrospun nanofibers and securing the edges through the use of solvent, glue, or heating. This technique allows one to use multiple, different layers, for example, a mesh of aligned fibers in the inner layer and a nonwoven mat of random fibers in the outer layer (Fig. 4F).[85] Since a mat made of random fibers has a larger porosity comparing to the aligned counterpart, the multilayered conduits would support better nutrient transport and cell outgrowth without compromising contact guidance. Recently, a biomimetic scaffold was fabricated by rolling electrospun nanofiber matrices in a concentric manner with an open central cavity to replicate bone marrow cavity as well as the lamellar structure of bone.[86] In this case, a rectangular strip of electrospun nanofibers was rolled around a 1-mm thick Teflon rod to produce the concentric structure. The compressive modulus of the scaffold was found to be in the mid-range of human trabecular bone. The porous structure also encouraged osteoblast infiltration and ECM secretion by mimicking the native structure of the bone.

5. Applications in regenerative medicine

5.1 Nerve injury repair

The recovery of injuries to both peripheral and central nervous systems can greatly benefit from the neural tissue engineering strategy that uses a scaffold or conduit to facilitate the re-growth of nerves.[87] The most severe injury to a peripheral nervous system (PNS) is the complete transection of the nerve fiber. After the injury, protease activity increases at the site of injury, giving rise to a series of degradation events at the distal ends of the injured nerve fiber.[88] In the central nervous system (CNS), the initial neurological damage provokes a series of cellular and biochemical responses, resulting in a secondary injury. The secondary injury prohibits nerve regeneration and causes more cell death, creating a cavity at the injury site and glial scar around the lesion.[89] Since the environment at the injured site discourages the elongation and re-innervation of axonal re-growth, CNS nerve repairs are more challenging than PNS nerve repairs.

The extension of a regenerating axon requires positive cues to be built within the scaffold. The growth cone at the tip of the axon cylindrically extends into the ECM searching for cues and retracts when inhibitory molecules are encountered or if no positive cues are found. It then transduces the guidance cues into intracellular signals for neurite extension and orientation. Conventional hydrogel scaffolds are isotropic, and hence they cannot provide any directional cues.[90] Microchannels, microridges, microgrooves, and stripes can provide topographical cues to direct neurite extension, but the dimension of these microstructures are on the same scale as the diameter of axons or cells and thus they are unable to guide sub-cellular events.[85] Electrospun nanofibers, on the other hand, are more physiologically relevant to the fibrous structures of native ECM of neural tissues and can thus interact intimately with the growth cones to provide contact guidance for directed neurite extension.

Many research groups have demonstrated that uniaxially aligned nanofibers can not only provide directional contact guidance, but also encourage longer axonal protrusion to bridge the severe nerve defect. Ramakrishna and co-workers have demonstrated that neurites sprouting from neonatal mouse cerebellum C17.2 NSCs ran parallel to the aligned PLLA fibers and axons of up to 100 μm were formed due to the enhanced contact guidance.[66] We also showed that the average length of the neurites projected from chicken primary DRG cultured on aligned nanofibers was ~1,100 μm, whereas this value was ~800 μm on random nanofibers.[81] Figure 5, A and B, shows a projection of the neurites from DRG cultured on aligned and random nanofibers, respectively. The neurites were stained with anti-neurofilament 200, which recognize an epitope present on neurofilaments 200 kDa. The anisotropy of a scaffold made of aligned nanofibers also encouraged the differentiation of ESCs towards a neural lineage.[81] CE3 mouse ESCs were induced to become neural progenitor cells by adding retinoic acid to embryoid body (EB) cultures, and after for 4 days the EBs were seeded onto electrospun nanofibers and allowed to differentiate. An increase in the proportion of neurons and neural precursor cells and a decrease in the proportion of astrocytes was found for aligned nanofibers compared to random nanofibers.[69] Neural guidance conduits (NGCs) with variations in both fiber organization and composition can be easily constructed by rolling and sealing non-woven mats of nanofibers. Leong and co-workers demonstrated that NGCs composed of axially aligned fibers were able to improve peripheral nerve regeneration across a 15-mm nerve defect compared with NGCs consisting of random or circumferentially aligned fibers.[91] Bellamkonda and co-workers examined the repair of a 17-mm nerve gap using a NGC fabricated by stacking 10–12 layers of electrospun nanofiber mats within two halves of a longitudinally split polysulfone tube. The results demonstrated that the aligned rather than the random construct successfully promoted regeneration of axons across the 17-mm nerve gap, re-innervated muscles, and formed new neuromuscular junctions.[92] We also compared the healing effects of conduits base on silicone tubes and conduits of electrospun nanofibers over 10-mm defects in the sciatic nerves of rats. Figure 5, C and D, shows the results 8 weeks post operation. The conduits based on electrospun nanofibers were composed of two layers, with aligned nanofibers as the inner layer and random nanofibers as the outer layer. Toluidine blue staining of cross sections of the regenerated nerves indicated that the two types of conduits were comparable to each other in terms of regenerative capacity. However, 3D isometric reconstruction images revealed much more uniform nerve regeneration in the conduit made of nanofibers, especially in the middle zone (see the insets). These results indicated that the aligned nanofibers on the inner surface of the conduit could facilitate the regeneration of nerve by providing guidance to neurite extension, while the porosity in wall was advantages for the transport of nutrients and metabolic waste. This type of conduit is promising for applications in peripheral nerve repair.[85]

The large surface area of a scaffold of electrospun nanofibers may provide superior cues for the differentiation of NSCs by accommodating a higher concentration of neurotrophic

factors. For example, aminolysation of the surface of PCL electrospun fibers with ethylene diamine improved the adhesion and migration of adult rat brain derived NSCs into the scaffold.[93] Fiber diameter is a significant factor in controlling the differentiation of NSCs. Reduction in diameter led to increased cell proliferation, spreading, and differentiation. A lower degree of cell aggregation was also reported for scaffolds made of nanofibers with smaller diameters.[94] Electrical stimulation has been recognized as another contributing factor for neurite sprouting. To this end, we fabricated a scaffold of conductive core-sheath nanofibers through a combination of electrospinning and aqueous polymerization. Specifically, electrospun nanofibers of PCL or PLLA were employed as templates to generate uniform sheaths of conductive polypyrrole (PPy) via *in situ* polymerization. Figure 5E shows a TEM image of hollow PPy tubes obtained by dissolving the core polymer. Electrical stimulation, when applied through the scaffolds of conductive core-sheath nanofibers, was found to further increase the maximum length of neurites for aligned samples by 47% relative to the controls with no electrical stimulation.[95] Figure 5F shows the synergetic effect of electrical stimulation and topographic guiding in promoting the uniaxial extension of neurites from DRG over long distances.

Although many efforts have been devoted to the field of nerve repair, challenges still exist. For example, the development of double-layered NGCs (with random nanofibers as the outer layer and the aligned nanofibers as the inner layer) has achieved some promising results,[96] but the central cavity in the NGCs fails to provide contact guidance for neuronal outgrowth and thus will probably lead to a mismatch between proximal and distal ends. An NGC that provides 3D contact guidance throughout the whole conduit has yet to be developed.

5.2 Dura mater repair

The dura mater is the outermost layer of the three meninges that surround the brain and the spinal cord. Its major function is to help retain the cerebrospinal fluid (CSF). Traumatic injury or surgical operation often leaves a defect in the dura mater, which needs to be covered by a dural substitute to prevent CSF leakage and promote the regeneration of dura tissue.[97] Materials that have been used as dural substitutes include native autografts, xenografts, and synthetic polymers. Whereas native autografts such as fascia lata work well as dural substitutes due to their low immunogenicity, their availability and the morbidity associated with the explanted sites severely limits their use.[98] Various xenologous collagen grafts, including bovine and ovine pericardium, have been developed as alternatives, but with limited success due to the risk of disease transmission and immunogenicity from animal-derived materials.[99] Other concerns such as low-tensile strength and rapid bioresorption also plague the use of xenologous collagen grafts. Scaffolds based on synthetic, biodegradable polymers have gained popularity in recent years because of their low cost, zero risk of disease transmission, and good mechanical properties. In particular, the high rate of cell infiltration and the ability to provide directional contact guidance have made nonwoven mats of electrospun nanofibers a new class of promising dural substitutes.

The regeneration rate of the injury site is a key factor in evaluating the efficacy of a dural substitute. Several prior studies have shown that cells cultured on scaffolds of uniaxially aligned nanofibers tend to migrate along the nanofibers.[100] Based on this observation, we developed nanofibers with radial alignment to specifically target dura mater repair and other applications involving wound closure. In a typical dural defect, the injured site is still surrounded by healthy, intact tissue. By accelerating the migration of dura fibroblasts from the periphery, it is possible to achieve fast closure for the dural defect. We have demonstrated that dural fibroblasts were able to cover the entire surface of a scaffold made of radially aligned fibers within 4 days, while a void still existed on a control based on random nanofibers, indicating a faster migration rate for the cells on radially aligned

nanofibers (Fig. 6, A and B).[69] An enlarged view of the center regions are shown Figure 6, C and D, where a void of cells can be clearly seen on the random scaffold.

Synthetic materials possess a range of advantages over collagen matrices: they are cost effective, mechanically strong, and less prone to diseases transfer. The ability to generate radially aligned topography distinguishes electrospinning from other techniques in the fabrication of dural substitutes. A current limitation of electrospun dural substitutes is that they are not suitable for small dural defects where on-lay transplantation (without suturing) is needed. Further research should include efforts to alter the surface chemistry of the electrospun nanofibers so that they can be used for both on-lay and in-lay purposes.

5.3 Tendon/ligament repair

Tendon (connecting muscle and bone) and ligament (connecting bone to bone) tissues are compositionally, structurally, and mechanically similar. Both tissues are loaded primarily in one direction and their ECM (mostly type I collagen) has a uniaxially aligned structure, leading to highly anisotropic mechanical properties.[101] Tendon/ligament has a low propensity for regeneration due to its high ECM density, collagen organization, and low vascularity.[102] The scar-mediated healing response of tendon/ligament and its inability to regenerate has led to the investigation of tissue engineering approaches to replace the damaged or diseased tissue.

Braided and knitted fabrics have been used as scaffolds for tendon/ligament repair. The major drawbacks of these constructs are the poor performance in mass transport, cell attachment, and cell infiltration.[103] Scaffolds based on electrospun nanofibers have started to gain popularity in the field of tendon/ligament repair not only because of the high porosity and high cell infiltration rate, but also due to the ease of generating uniaxial alignment to mimic the anisotropic structure of native tissues. Fibroblasts and BMSCs are often cultured on aligned nanofibers to generate a cell-seeded scaffold. Ouyang and co-workers found that, when seeded on aligned PLLA fibers, human tendon progenitor cells (hTSPCs) oriented themselves along the direction of the fibers and expressed higher level of tendon specific genes than those seeded on random fibers.[18] Figure 7, A and B, shows alkaline phosphatase (ALP) stating of hTSPCs cultured on scaffolds consisting of aligned and random fibers, respectively, in normal osteogenic induction media for 2 weeks. Figure 7, C and D, shows alizarin red S staining of hTSPCs cultured on aligned and random scaffolds under the same conditions. These results indicated the pluripotent nature of the hTSPCs. Figure7, E and F, shows Masson's trichrome staining of collagen fibers formed on the fibrous scaffolds after 6 weeks *in vivo*. Whereas aligned fibers induced the formation of aligned collagen fibrils similar to the native system, random fibers resulted in the formation of haphazard collagen fibrils. Shin and co-workers investigated the influence of nanofiber alignment and the direction of mechanical strain stimulation on ECM production of human anterior cruciate ligament fibroblast (HLF).[104] The HLFs on the aligned nanofibers were spindle-shaped and oriented in the direction of the nanofibers. Significantly more collagen was synthesized on aligned fibers than on random fibers. After culture at 5% uniaxial strain for 24 h at a frequency of 12 cycles per min, the HLFs produced more collagen on the longitudinally stretched scaffolds than on those stretched in the transverse direction. Similar results were obtained by Lu and co-workers, who cultured human rotator cuff fibroblasts on scaffolds of aligned and random PLGA nanofibers.[105] Distinct integrin expression profiles on these two scaffolds were observed, with higher expression of integrin on aligned nanofibers. Quantitative analysis revealed that cell alignment, distribution, and matrix deposition conformed to nanofiber alignment and that the observed differences were maintained over time. Mechanical properties of the aligned nanofiber scaffolds were significantly higher than those of the unaligned, and although the scaffolds degraded in vitro, physiologically relevant mechanical properties were maintained.

In addition to fiber alignment, the crimped nature of collagen fibrils in tendon/ligament is an important feature that should be considered when preparing nanofiber scaffolds for application in tendon/ligament repair. Fiber crimp leads to relatively high extension under low loads, providing the characteristic non-linear mechanical behavior of tendon and ligaments and possibly shielding cells from high shear stresses. Electrospun nanofibers could be induced to crimp upon removal from a mandrel that rotates at a very high speed (Fig. 7D). The crimped morphology could be retained for at least 4 weeks in PBS at 37 °C (Fig. 7E). The crimping effect was determined to be a result of the residual stresses resident in the fibers during the fiber alignment process. The same group also produced crimp in electrospun nanofibers by using a temperature higher than the glass-transition temperature of the polymer. The resultant crimped fibers exhibited a long toe region in their stress-strain curve, reproducing a characteristic of the collagen fibrils in native tendon/ligament.[106]

The ease of producing uniaxial alignment represents a major advantage for electrospinning in fabricating scaffolds for tendon/ligament repair. Growing interest has been focused on generating crimped structures with tension bearing capacity similar to that of native tendon/ligament. While the shape of the stress-strain curve for a scaffold made of crimped, electrospun nanofibers resembles that of native tendon/ligament, the magnitude of the curve for these constructs is much smaller than that of native tissue. The insufficient mechanical properties for the demanding mechanical physiological conditions of tendons and ligaments may lead to premature failure of the healing tendon/ligament. Future work should focus on improving the mechanical properties of aligned and crimped nanofiber scaffolds.

5.4 Tendon-to-bone insertion site repair

The tendon-to-bone insertion (the enthesis) can generally be characterized as either fibrous or fibrocartilagious.[107] At a fibrous insertion, a tendon attaches to the bone at an acute angle through collagen fibers that extend directly to the bone. In contrast, a fibrocartilagious insertion is characterized by a functionally graded transitional zone of tendon, followed by uncalcified fibrocartilage, mineralized fibrocartilage, and bone.[108] The transitional zone exhibits a gradual change in mineral content, spatial organization, cell type, and signaling molecules. While the tendon tissue is made up of densely packed and well-aligned collagen fibrils, the bone tissue is made up of less oriented and highly mineralized collagen fibrils. No sharp boundary exists between the tendon and bone; rather, a functionally graded architecture connects the very different tissues, mitigating stress concentrations and enabling the transmission of forces.

Tendon-to-bone insertion repair is a well-known clinical challenge. For example, surgical repair of the injured rotator cuff usually involves suturing the torn tendon to the humeral head.[109] Although the tendon is re-attached to its anatomic footprint, the functionally graded transitional tissue is not regenerated and the repair often fails. In order to improve outcomes after tendon-to-bone repair, tissue engineers seek to develop a scaffold that recapitulates the native, graded structure of fibrocartilagious tendon-to-bone insertion. Such a scaffold may facilitate the surgical repair and provide functional recovery of a robust attachment between the repaired tendon and bone. Two different methods have been demonstrated for fabricating scaffolds to be used for tendon-to-bone repair. In the first method, stratified scaffolds were fabricated by co-culture of multiple types of cells.[110] The expectation is that the interactions among different cell types would eventually result in cell-mediated development of a functional insertion. In the second method, stem cells are seeded onto a graded scaffold with variation in surface chemistry such as the concentration of bioactive molecules or mechanical properties.[111] The argument is that the stem cells will respond to the different local stimuli, differentiating into various types of cells and thus generating a functional insertion.[112] The fabrication of a scaffold with a graded coating of mineral on electrospun nanofibers falls into the second approach.

The potential use of electrospun nanofiber scaffolds in addressing tendon-to-bone insertion repair has been investigated by several groups.[111b,113] In one study, we gradually added 10 times concentrated simulated body fluid (10SBF) into a glass vial containing a piece of the electrospun nanofiber scaffold (Fig. 8A). A mineral gradient was formed along the length of the scaffold due to the difference in immersion time along the vertical direction. Significantly, the gradient in mineral content resulted in a gradient in stiffness for the scaffold and thus the MC3T3 mouse preosteoblasts were found to preferentially attach to the end higher in mineralization.[111b] Figure 8, B and C, show SEM images of the scaffold. The fluorescence micrographs in Figure 8, D and E, indicate that the MC3T3 cells had a low affinity for the unmineralized end of the scaffold and a high affinity for the highly mineralized end of the scaffold.

We also fabricated scaffolds with an "aligned-to-random" transition for the electrospun PLGA nanofibers that could mimic the structural organization of collagen fibers at the tendon-to-bone insertion site (Fig. 8F). Figure 8G shows an SEM image taken from the boundary between the aligned and random nanofibers. As shown in Figure 8H, tendon fibroblasts cultured on such a scaffold exhibited highly organized and haphazardly oriented morphologies, on the aligned and random portions of the scaffold, respectively.[113a]

Gradation in surface-attached bioactive molecules can also be achieved by adding a solution gradually. For example, Chen and co-workers fabricated a poly(methyl glutarimide) scaffold with graded fibronectin by placing the scaffold of electrospun nanofibers vertically in a container, into which a fibronectin solution was added in a controlled manner.[113b] They also observed a positive correlation between the population of NIH/3T3 fibroblasts and the concentration of fibronectin. A technique called twin-screw extrusion/electrospinning was utilized by Kalyon and co-workers to fabricated scaffolds of electrospun PCL nanofibers with gradation in β-tricalcium phosphate (β-TCP) concentration along the thickness direction.[113c, d] The technique involved the use of a twin screw extruder with fully intermeshing and rotating screws integrated with a multichannel spinneret, which was connected to a high-voltage power supply. Injection ports on the side surface of the barrel enabled the introduction of β-TCP continuously. The screws were rotated to allow for mixing. The feeding rate for the β-TCP solution was gradually increased over time. The resultant scaffold had a gradient in β-TCP concentration along the thickness direction. The graded scaffold was then seeded and cultured with MC3T3. After 4 weeks, the tissue construct showed continuous gradation in ECM, including both collagen synthesis and mineralization.[113d]

These studies demonstrate that electrospinning is a promising approach to the fabrication of graded scaffolds with physical and chemical properties similar to the natural ECM of the tendon-to-bone insertion. However, this technique is still in the early stages of development. Most of the studies to date have focused on the establishment of new fabrication systems to produce the desired gradients, whereas the differentiation of stem cells such as bone mesenchymal stem cells (BMSCs) on such scaffolds has not yet been systematically investigated. *In vivo* studies should also be carried out to assess the efficacy of such graded scaffolds in tendon-to-bone insertion repair.

6. Concluding remarks

Electrospinning is a remarkably simple and versatile technique. This technique can generate nanofibers on a large scale while also allowing one to tailor many aspects of the resulting scaffold: *i*) the fiber diameter can easily be controlled by varying the concentration of the solution, ejection rate, applied voltage, and the distance between the spinneret and the collector; *ii*) the nanofibers can be readily fabricated with a hollow or core-sheath structure

by altering the configuration of the spinneret; *iii*) the nanofibers can be made highly porous by inducing a phase separation between the polymer and the solvent;[114] *iv*) the nanofibers can be aligned into a rich variety of structures by using specially designed collectors; and *v*) the nanofibers can be stacked and/or folded to form complex structures or architectures. Electrospinning has been successfully applied to a wide range of biomaterials, including natural proteins (e.g., collagen and elastin) and synthetic polymers such as PLGA, PCL, PLA, and PGA that have been approved by Federal Drug Administration (FDA) as biocompatible and biodegradable materials for clinical use. Its capabilities have also been extended to include inorganic materials such as hydroxyapatite (HA), bioactive glasses, and their composites with polymers.[115] Because of the high porosity and large surface area, a scaffold derived from electrospun nanofibers can mimic the hierarchical structure of ECM that is critical for cell attachment and spreading as well as nutrient/waste transportation. If necessary, the nanofibers can be further functionalized via encapsulation or attachment of bioactive species such as ECM proteins, enzymes, DNAs, and growth factors to better control the proliferation and differentiation of cells seeded on the scaffolds. These attributes make electrospun nanofibers well-suited as scaffolds for regenerative medicine.

Whereas impressive progress has been made in applying electrospun nanofibers as scaffolds for regenerative medicine, challenges still exist. Low cell infiltration rates remain one of the most significant hurdles that must be cleared before this technology can be applied to most *in vivo* systems. Although the porosity of a nanofiber-based scaffold can be enlarged to facilitate cell infiltration by incorporating a sacrificial component, the mechanical properties and integrity of the scaffold are often compromised. Moreover, due to the abundance of nutrients at the surface of the scaffold, it is likely that cells will prefer to stay on the surface without migrating into the bulk. Direct electrospinning of live cells has emerged as a novel technique to address this challenge. To this end, Jayasinghe and co-workers used a coaxial electrospinning method to enable the flow of highly concentrated cellular suspension in the inner capillary while the outer needle accommodated the flow of a poly(dimethylsiloxane) (PDMS) medium.[116] A large population of the cells remained viable post-electrospinning for a relatively long period of time, as assessed by flow cytometry.

Another technical challenge for the application of electrospun nanofiber scaffolds is that the diameter of the fibers cannot be easily reduced to a scale below 100 nm, which is the upper limit of native ECM fibers. In particular, the nanoscale size is difficult to achieve for the natural and synthetic polymers commonly used for tissue engineering applications. To better mimic the ECM, it is desirable to produce fibers with diameters thinner than 100 nm, preferably in the range of 10–50 nm. When the size of electrospun fibers is reduced, an additional issue will arise in that the porosity of the scaffold will decrease accordingly. There is a strong need to develop a method capable of generating fibers with diameters identical to that of native ECM fibers while maintaining a high porosity and thus high rates for cell infiltration and mass transport. As a better understanding of the electrospinning process is achieved through theoretical modeling, it is expected that all these technical problems will be solved in the near future.

References

1. Badylak SF, Taylor D, Uygun K. Ann Rev Biomed Eng. 2011; 13:27. [PubMed: 21417722]
2. Langer R, Vacanti JP. Science. 1993; 260:920. [PubMed: 8493529]
3. Ikada Y. J R Soc Interface. 2006; 3:589. [PubMed: 16971328]
4. http://www.organdonor.gov
5. Badylak SF, Nerem RM. Proc Natl Acad Sci USA. 2010; 107:3285. [PubMed: 20181571]
6. Khademhosseini A, Vacanti JP, Langer R. Sci Am. 2009; 300:64. [PubMed: 19438051]

7. (a) Ott HC, Matthiesen TS, Goh S-K, Black LD, Kren SM, Netoff TI, Taylor DA. Nat Med. 2008; 14:213. [PubMed: 18193059] (b) Petersen TH, Calle EA, Zhao L, Lee EJ, Gui L, Raredon MB, Gavrilov K, Yi T, Zhuang ZW, Breuer C, Herzog E, Niklason LE. Science. 2010; 329:538. [PubMed: 20576850]

8. Kelleher CM, Vacanti JP. J R Soc Interface. 2010; 7:S717. [PubMed: 20861039]

9. Dvir T, Timko BP, Kohane DS, Langer R. Nat Nanotech. 2011; 6:13.

10. Prestwich GD. J Cell Biochem. 2007; 101:1370. [PubMed: 17492655]

11. Lutolf MP, Gillbert PM, Blau HM. Nature. 2009; 462:433. [PubMed: 19940913]

12. Madurantakam PA, Cost CP, Simpson DG, Bowlin GL. Nanomedicine. 2009; 4:193. [PubMed: 19193185]

13. Agarwal S, Wendorff JH, Greiner A. Adv Mater. 2009; 21:3343. [PubMed: 20882501]

14. Pham QP, Sharma U, Mikos AG. Tissue Eng. 2006; 12:1197. [PubMed: 16771634]

15. Frenst A, Chronakis IS. Curr Opin Colloid Interface Sci. 2003; 8:64.

16. Schnell E, Klinkhammer K, Balzer S, Brook G, Klee D, Dalton P, Mey J. Biomaterials. 2007; 28:3012. [PubMed: 17408736]

17. Zong X, Bien H, Chung CY, Yin L, Fang D, Hsiao BS, Chu B, Entcheva E. Biomaterials. 2005; 26:5330. [PubMed: 15814131]

18. Yin Z, Chen X, Chen JL, Shen WL, Nguyen TMH, Gao L, Ouyang HW. Biomaterials. 2010; 31:2163. [PubMed: 19995669]

19. Lu H, Feng Z, Gu Z, Liu C. J Mater Sci Mater Med. 2009; 20:1937. [PubMed: 19399594]

20. Hashi CK, Zhu Y, Yang G-Y, Young WL, Hsiao BS, Wang K, Chu B, Li S. Proc Natl Acad Sci USA. 2007; 104:11915. [PubMed: 17615237]

21. Schnell E, Klinkhammer K, Balzer S, Brook G, Klee D, Dalton P, Mey J. Biomaterials. 2007; 28:3012. [PubMed: 17408736]

22. Xin X, Hussian M, Mao JJ. Biomaterials. 2007; 28:316. [PubMed: 17010425]

23. Burger C, Hsiao BS, Chu B. Ann Rev Mater Res. 2006; 36:333.

24. Bergsma EJ, Rozema FR, Bos RRM, Bruijin WCD. J Oral Maxil Surg. 1993; 51:666.

25. (a) Matthews JA, Wnek GE, Simpson DG, Bowlin GL. Biomacromol. 2002; 3:232.(b) Buttafocoa L, Kolkmana NG, Engbers-Buijtenhuijsa P, Poota AA, Dijkstraa PJ, Vermesa I, Feijen J. Biomaterials. 2006; 5:724.

26. Barnes CP, Pemble CW, Brand DD, Simpson DG, Bowlin GL. Tissue Eng. 2007; 13:1593. [PubMed: 17523878]

27. Shields KJ, Beckman MJ, Bowlin GL, Wayne JS. Tissue Eng. 2004; 10:1510. [PubMed: 15588410]

28. (a) Choi JS, Lee SJ, Christ GJ, Atala A, Yoo JJ. Biomaterials. 2008; 19:2899. [PubMed: 18400295] (b) Wang G, Hu X, Lin W, Dong C, Wu H. In Vitro Cell Dev Biol Anim. 2011; 47:234. [PubMed: 21181450] (c) Jeong SI, Kim SY, Cho SK, Chong MS, Kim KS, Kim H, Lee SB, Lee YM. Biomaterials. 2007; 28:1115. [PubMed: 17112581]

29. Powell HM, Boyce ST. Tissue Eng Part A. 2009; 15:2177. [PubMed: 19231973]

30. Ji W, Sun Y, Yang F, Beucken JJJV, Fan M, Chen Z, Jansen JA. Pharm Res. 2011; 28:1259. [PubMed: 21088985]

31. (a) Li C, Vepari C, Jin HJ, Kim HJ, Kaplan DL. Biomaterials. 2006; 27:3115. [PubMed: 16458961] (b) Schneider A, Wang XY, Kaplan DL, Garlick JA, Egles C. Acta Biomater. 2009; 5:2570. [PubMed: 19162575] (c) Sahoo S, Ang LT, Goh JC, Toh SL. J Biomed Mater Res A. 2009; 93:1539. [PubMed: 20014288]

32. Varkey M, Gittens SA, Uludag H. Expert Opin Drug Deliv. 2004; 1:19. [PubMed: 16296718]

33. Casper CL, Yamaguchi N, Kiick KL, Rabolt JF. Biomacrobolecules. 2005; 6:1998.

34. Yoo HS, Park TG. Adv Drug Deliv Rev. 2009; 61:1033. [PubMed: 19643152]

35. Sah H. PDA J Pharm Sci Tech. 1999; 53:3.

36. Nie H, Soh BW, Fu YC, Wang CH. Biotechnol Bioeng. 2008; 99:223. [PubMed: 17570710]

37. Jiang W, Schwendeman SP. Pharm Res. 2001; 18:878. [PubMed: 11474795]

38. Chew SY, Wen Y, Dzenis Y, Leong KW. Curr Pharm Des. 2006; 12:4751. [PubMed: 17168776]

39. Xie J, Li X, Xia Y. Macromol Rapid Commun. 2008; 29:1775. [PubMed: 20011452]

40. Jo E, Lee S, Kim KT, Won YS, Kim H-S, Cho EC, Jeong U. Adv Mater. 2009; 21:968.

41. (a) Luu YK, Kim K, Hsiao BS, Chu B. J Control Release. 2003; 89:341. [PubMed: 12711456] (b) Zeng J, Aigner A, Czubayko F, Kissel T, Wendorff JH, Greiner A. Biomacromolecules. 2005; 6:1484. [PubMed: 15877368] (c) Chew SY, Wen J, Yim EK, Leong KW. Biomacromolecules. 2005; 6:2017. [PubMed: 16004440] (d) Zhang YZ, Wang X, Feng Y, Li J, Lim CT, Ramakrishna S. Biomacromolecules. 2006; 7:1049. [PubMed: 16602720] (e) Jiang H, Hu Y, Li Y, Zhao P, Zhu K, Chen W. J Control Release. 2005; 108:237. [PubMed: 16153737]

42. Huang X, Brazel CS. J Control Release. 2001; 73:121. [PubMed: 11516493]

43. Choi JS, Leong KW, Yoo HS. Biomaterials. 2008; 29:587. [PubMed: 17997153]

44. Middleton JC, Tipton AJ. Biomaterials. 2000; 21:2335. [PubMed: 11055281]

45. (a) Gilding DK, Reed AM. Polymer. 1979; 20:1459.(b) Loo JSC, Ooi CP, Boey FYC. Biomaterials. 2005; 26:1359. [PubMed: 15482823]

46. Pietrzak WS, Sarver DR, Verstynen BS. J Craniofacial Surg. 1997; 2:87.

47. (a) Therin M, Christel P, Li S, Garreau H, Vert M. Biomaterials. 1992; 13:594. [PubMed: 1391406] (b) Athanasiou KA, Schmitz JB, Agrawal CM. Tissue Eng. 1998; 4:53.

48. (a) Browning A, Chu CC. J Biomed Mater Res. 1986; 20:613. [PubMed: 3011808] (b) Ginde RM, Gupta RK. J Appl Polym Sci. 1987; 33:2411.

49. Kakade MV, Givens S, Gardner K, Lee KH, Chase DB, Rabolt JF. J Am Chem Soc. 2007; 129:2777. [PubMed: 17302411]

50. Mauck RL, Baker BM, Nerurkar NL, Burdick JA, Li W-J, Tuan RS, Elliot DM. Tissue Eng Part B. 2009; 15:171.

51. Li WJ, Cooper JA, Mauck RL, Tuan RS. Acta Biomater. 2006; 2:377. [PubMed: 16765878]

52. Inai R, Kotaki M, Ramakrishna S. Nanotechnology. 2005; 16:208. [PubMed: 21727424]

53. Chew SY, Hugnagel TC, Lim CT, Leong KW. Nanotechnology. 2006; 17:3880. [PubMed: 19079553]

54. Moffat KL, Spalazzi AS-P, Doty SB, Levine WN, Lu HH. Tissue Eng Part A. 2009; 15:115. [PubMed: 18788982]

55. Nerurkar NL, Baker BM, Sen S, Wible EE, Elliott DM, Mauck RL. Nat Mater. 2009; 8:986. [PubMed: 19855383]

56. Liu W, Yeh Y-C, Lipner J, Xie J, Sung H-W, Thomopoulos S, Xia Y. Langmuir. 2011; 27:9088. [PubMed: 21710996]

57. Engler AJ, Sen S, Sweeney HL, Discher DE. Cell. 2006; 126:677. [PubMed: 16923388]

58. Huang S, Ingber DE. Nat Cell Biol. 1999; 1:131.

59. Tan EPS, Lim CT. J Biomed Mater Res A. 2006; 77:526. [PubMed: 16489588]

60. (a) Flanagan LA, Ju YE, Marg B, Osterfield M, Janmey PA. NeuroReport. 2002; 13:2411. [PubMed: 12499839] (b) Ingber DE. Proc Natl Acad Sci USA. 2003; 100:1472. [PubMed: 12578965]

61. Martins A, Aranjo JV, Neves NM. Nanomedicine. 2007; 2:929. [PubMed: 18095855]

62. Eichhorn J, Sampson WW. J R Soc Interface. 2005; 2:309. [PubMed: 16849188]

63. Nam J, Huang Y, Agarwal S, Lannutti J. Tissue Eng. 2007; 13:2249. [PubMed: 17536926]

64. (a) Zhang Y, Ouyang H, Lim CT, Ramakrishna S, Huang ZM. J Biomed Mater Res B Appl Biomater. 2005; 72:156. [PubMed: 15389493] (b) Kidoaki S, Kwon IK, Matsuda T. Biomaterials. 2005; 26:37. [PubMed: 15193879] (c) Baker BM, Gee AO, Metter RB, Nathan AS, Marklein RA, Burdick JA, Mauck RL. Biomaterials. 2008; 29:2348. [PubMed: 18313138]

65. Blakeney BA, Tambralli A, Anderson JM, Andukuri A, Lim D-J, De DR, Jun H-W. Biomaterials. 2011; 32:1583. [PubMed: 21112625]

66. Yang F, Murugan R, Wang C, Ramakrishna S. Biomaterials. 2005; 26:2603. [PubMed: 15585263]

67. Xie J, Willerth SM, Li X, MacEwan MR, Rader A, Sakiyama-Elbert SE, Xia Y. Biomaterials. 2009; 30:354. [PubMed: 18930315]

68. Nisbet DR, Forsythe JS, Shen W, Finkelstein DI, Horne MK. J Biomater Appl. 2008; 24:7. [PubMed: 19074469]

69. Xie J, MacEwan MR, Ray WA, Liu W, Siewe DY, Xia Y. ACS Nano. 2010; 4:5027. [PubMed: 20695478]

70. (a) Barnes CP, Sell SA, Boland ED, Simpson DG, Bowlin GL. Adv Drug Delivery Rev. 2007; 59:1413.(b) Teo WE, Ramakrishna S. Nanotechnology. 2006; 17:R89. [PubMed: 19661572]

71. Theron A, Zussman E, Yarin AL. Nanotechnology. 2001; 12:384.

72. Sundaray B, Subramanian V, Natarajan TS, Xiang RZ, Chang CC, Fann WS. Appl Phys Lett. 2004; 84:1222.

73. Kessick R, Fenn J, Tepper G. Polymer. 2004; 45:2981.

74. Li D, Wang Y, Xia Y. Nano Lett. 2003; 3:1167.

75. Li D, Xia Y. Adv Mater. 2004; 16:1151.

76. Naraghi M, Arshad SN, Chasiotis I. Polymer. 2011; 52:1612.

77. Li D, Wang Y, Xia Y. Adv Mater. 2004; 16:361.

78. Xie J, Liu W, MacEwan MR, Yeh Y-C, Thomopoulos S, Xia Y. Small. 2011; 7:293. [PubMed: 21294253]

79. Yang D, Lu B, Zhao Y, Jiang X. Adv Mater. 2007; 19:3702.

80. Liu Y, Zhang X, Xia Y, Yang H. Adv Mater. 2010; 22:2454. [PubMed: 20376855]

81. Xie J, MacEwan MR, Li X, Sakiyama-Elbert SE, Xia Y. ACS Nano. 2009; 3:1151. [PubMed: 19397333]

82. Yang X, Shah JD, Wang H. Tissue Eng Part A. 2009; 15:945. [PubMed: 18788981]

83. Teo WE, Ramakrishna S. Nanotechnology. 2005; 16:1878.

84. Zhang D, Chang J. Nano Lett. 2008; 8:3283. [PubMed: 18767890]

85. Xie J, MacEwan MR, Schwarz AG, Xia Y. Nanoscale. 2010; 2:35. [PubMed: 20648362]

86. Deng M, Kumbar SG, Nair LS, Weikel AL, Allcock HR, Laurencin CT. Adv Funct Mater. 2011; 21:2641.

87. Schmidt CE, Leach JB. Ann Rev Biomed Eng. 2003; 5:293. [PubMed: 14527315]

88. Jacobson S, Guth L. Experim Neurol. 1965; 11:48.

89. Thuret S, Moon LDF, Gage FH. Nat Rev Neurosci. 2006; 7:628. [PubMed: 16858391]

90. (a) Nisbet DR, Crompton KE, Horne MK, Finkelstein DI, Forsythe JS. J Biomed Mater Res Part B. 2007; 87:251.(b) Nisbet DR, Compton KE, Hamilton SD, Shirwakawa S, Prankerd RJ, Finkelstein DI, Horne MK, Forsythe JS. Biophys Chem. 2005; 121:14. [PubMed: 16406645]

91. Chew SY, Mi R, Hoke A, Leong KW. Adv Funct Mater. 2007; 17:1288. [PubMed: 18618021]

92. Kim Y, Haftel VK, Kumar S, Bellamkonda RV. Biomaterials. 2008; 29:3117. [PubMed: 18448163]

93. Nisbet DR, Yu LMY, Zahir T, Forsythe JS, Shoichet MS. J Biomat Sci Polym E. 2008; 19:623.

94. Christopherson GT, Song H, Mao H. Biomaterials. 2008; 30:556. [PubMed: 18977025]

95. Xie J, MacEwan MR, Willerth SM, Li X, Moran DW, Sakiyama-Elbert SE, Xia Y. Adv Func Mater. 2009; 19:2312.

96. Zhu Y, Wang A, Patel S, Kurpinski K, Diao E, Bao X, Kwong G, Young WL, Li S. Tissue Eng Part C. 2011; 17:705.

97. Narotam PK, Qiao F, Nathoo N. J Neurosurg. 2009; 111:380. [PubMed: 19199453]

98. Dufrane D, Marchal C, Cornu O, Raftopoulos C, Delloye C. J Neurosurg. 2003; 98:1198. [PubMed: 12816264]

99. (a) Anson JA, Marchand EP. Neurosurgery. 1996; 39:764. [PubMed: 8880771] (b) Parizek J, Husek Z, Mericka P. J Neurosurg. 1996; 84:508. [PubMed: 8609566]

100. Liu Y, Franco A, Huang L, Gersappe D, Clark RAF, Rafailovich MH. Exp Cell Res. 2009; 315:2544. [PubMed: 19464288]

101. Li WJ, Mauck RL, Cooper JA, Yuan X, Tuan RS. J Biomech. 2007; 40:1686. [PubMed: 17056048]

102. Vunjak G, Altman G, Horan R, Kaplan DL. Annu Rev Biomed Eng. 2004; 6:131. [PubMed: 15255765]

103. Sahoo S, Ouyang H, Goh JCH, Tay TE, Toh SL. Tissue Eng. 2006; 12:91. [PubMed: 16499446]

104. Lee CH, Shin HJ, Cho IH, Kang Y-M, Kim IA, Park K-D, Shin JW. Biomaterials. 2005; 26:1261. [PubMed: 15475056]

105. Moffat KL, Kwei AS-P, Spalazzi JP, Doty SB, Levine WN, Lu HH. Tissue Eng Part A. 2006; 15:115. [PubMed: 18788982]

106. Surrao DC, Hayami JWS, Waldman SD, Amsden BG. Biomacromolecules. 2010; 11:3624. [PubMed: 21047054]

107. Woo SL, Buckwalter JA. J Orthop Res. 1988; 6:907. [PubMed: 3171771]

108. Benjamin M, Ralphs JR. J Anat. 1998; 193:481. [PubMed: 10029181]

109. Galatz LM, Ball CM, Teefey SA. J Bone Joint Surg Am. 2004; 86:219. [PubMed: 14960664]

110. (a) Dormer NH, Berkland CJ, Detamore MS. Ann Biomed Eng. 2010; 38:2121. [PubMed: 20411333] (b) Spalazzi JP, Doty SB, Moffat KL, Levine WN, Lu HH. Tissue Eng. 2006; 12:3497. [PubMed: 17518686]

111. (a) Phillips JE, Burns KL, Le Doux JM, Guldberg RE, Garcis AJ. Proc Natl Acad Sci USA. 2008; 105:12170. [PubMed: 18719120] (b) Li X, Xie J, Lipner J, Yuan X, Thomopoulos S, Xia Y. Nano Lett. 2009; 9:2763. [PubMed: 19537737]

112. Smith L, Thomopoulos S. US Musculoskeletal Rev. 2011; 6:11.

113. (a) Xie J, Li X, Lipner J, Manning CN, Schwartz AG, Thomopoulos S, Xia Y. Nanoscale. 2010; 2:923. [PubMed: 20648290] (b) Shi J, Wang L, Zhang F, Li H, Lei L, Liu L, Chen Y. ACS Appl Mater Interfaces. 2010; 2:1025. [PubMed: 20423122] (c) Erisken C, Kalyon DM, Wang H. Nanotechnology. 2008; 19:165302. [PubMed: 21825641] (d) Erisken C, Kalyon DM, Wang H. Biomaterials. 2008; 29:4065. [PubMed: 18649939]

114. McCann J, Marquez M, Xia Y. J Am Chem Soc. 2006; 128:1436. [PubMed: 16448099]

115. Li D, McCann J, Marquez M, Xia Y. J Am Ceram Soc. 2006; 89:1869.

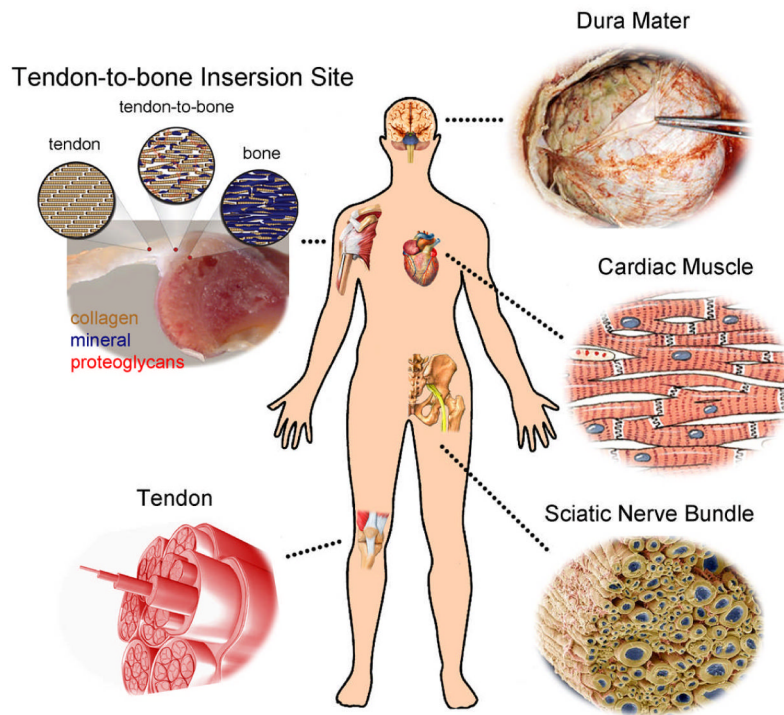116. Jayasinghe SN, Irvine S, MacEwan JR. Nanomedicine. 2007; 2:555. [PubMed: 17716138]

Figure 1.
Illustration of some typical examples of tissues in the human body whose regeneration would benefit from the use of nanofiber-based scaffolds with anisotropic structures that could be readily fabricated by electrospinning.
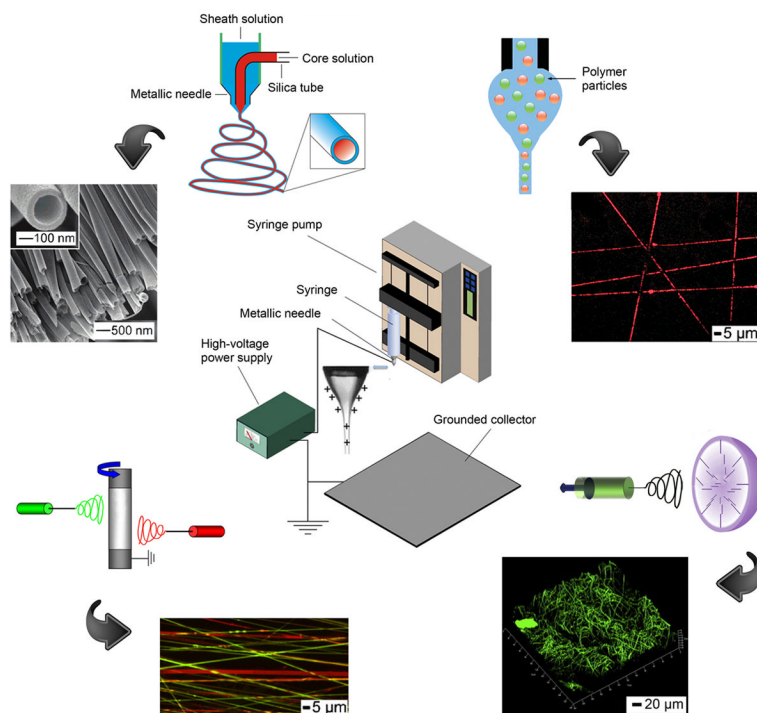
Figure 2.
Illustration of different variants of the electrospinning technique. (Center) A typical setup for electrospinning. (Top left) Electrospinning with a co-axial spinneret and SEM images of the corresponding hollow nanofibers. (Top right) Electrospinning with a mixture of polymer solution and polymer particles and a fluorescence image showing encapsulation of the polymer particles in the fibers. (Bottom left) Electrospinning with dual spinnerets and a fluorescence image showing a nonwoven mat containing two different types of polymer nanofibers. (Bottom right) Electrospinning with a hemispheral bowl collector and a confocal fluorescence image illustrating a typical cotton-ball like scaffold of fibers. Reproduced with permission: (top left) from Ref. [39], copyright 2008 Wiley-VCH; (top right) from Ref. [40], copyright 2009 Wiley-VCH; (bottom left) from Ref. [64c], copyright 2008 Elsevier; and (bottom right) from Ref. [65], copyright 2011 Elsevier.
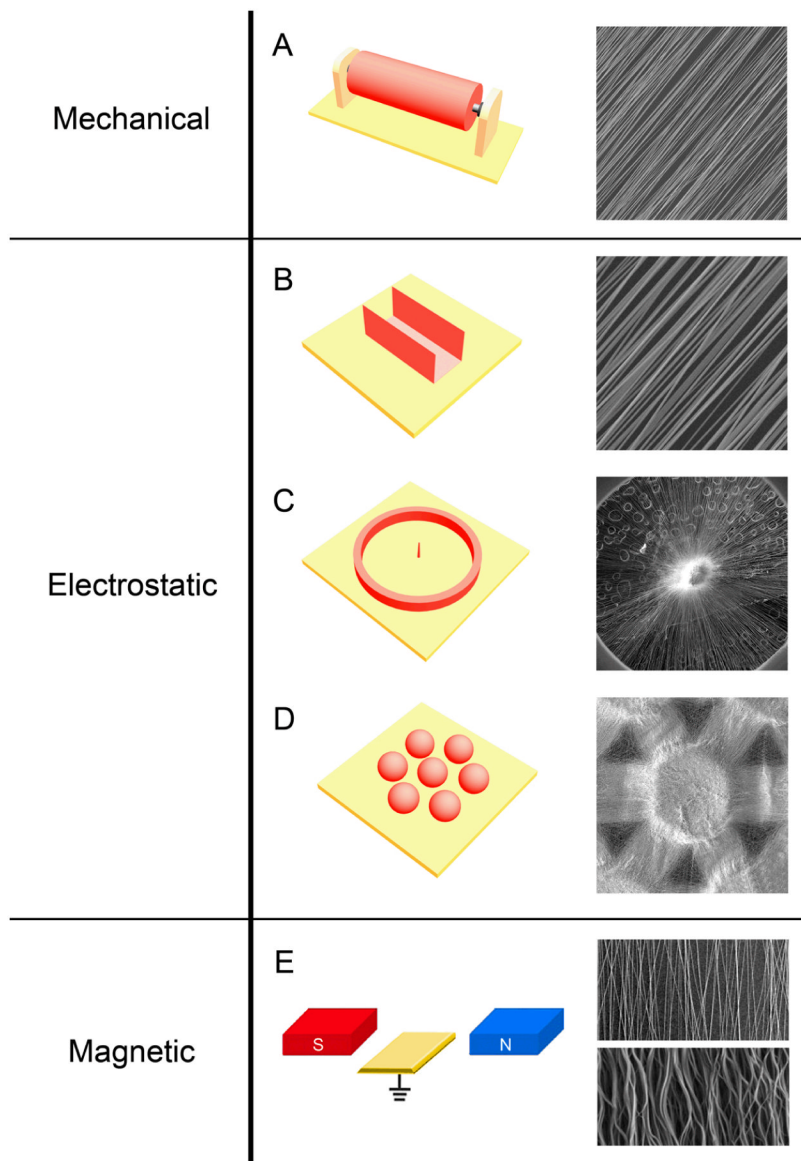
Figure 3.
Controlling the alignment of electrospun nanofibers using three different forces: *i*) mechanical forces through the use of a rotating mandrel (A); *ii*) electrostatic forces through the use of a metallic staple (B), a metallic ring with a metallic pin in the center (C), and an array of metallic beads (D); and *iii*) magnetic forces through the use of a pair of permanent magnets (E). The SEM images in the right column show typical morphologies of the aligned nanofibers collected using the different methods. The yellow plates are grounded conductive electrodes. Reproduced with permission: (C) from Ref. [69], copyright 2010 American Chemical Society; (D) from Ref. [78], copyright 2011 Wiley-VCH; and (E) from Ref. [80], copyright 2010 Wiley-VCH.
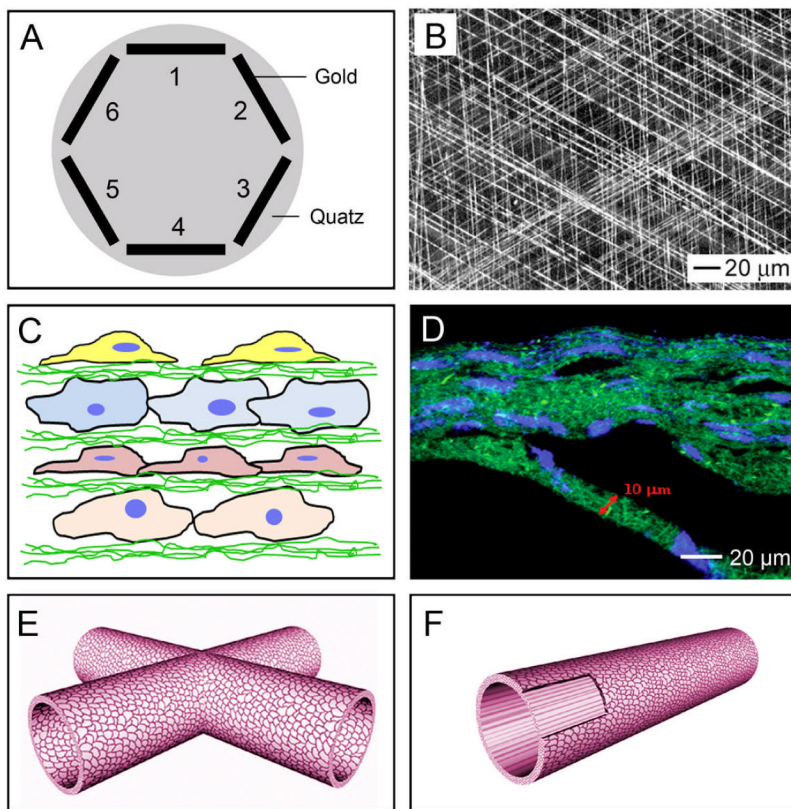
Figure 4.
Scaffolds of electrospun nanofibers with complex structures or architectures. A) A multi-electrode collector where different pairs of electrodes were grounded sequentially (e.g., 1/4, 2/5, and then 3/6) to produce a multi-layered scaffold. (B) SEM image of a tri-layered scaffold with the nanofibers in each layer rotated by 120 degrees. C) Encapsulation of cells in between nonwoven mats of nanofibers by alternating depositions of fibers and cells. D) Fluorescence micrograph showing a construct composed of alternating layers of fibers and cells, where the fibers were labeled with fluorescein isothiocyanate (FITC) to give a green color and the nuclei of cells were stained with 4′,6-diamidino-2-phenylindole (DAPI) for a blue color. E, F) Tubular conduits fabricated from non-woven mats of nanofibers. Reproduced with permission: (B) from Ref. [75], copyright 2004 Wiley-VCH; (D) from Ref. [82], copyright 2009 Mary Ann Liebert; and (E, F) from Ref. [85], copyright 2010 RSC Publishing.
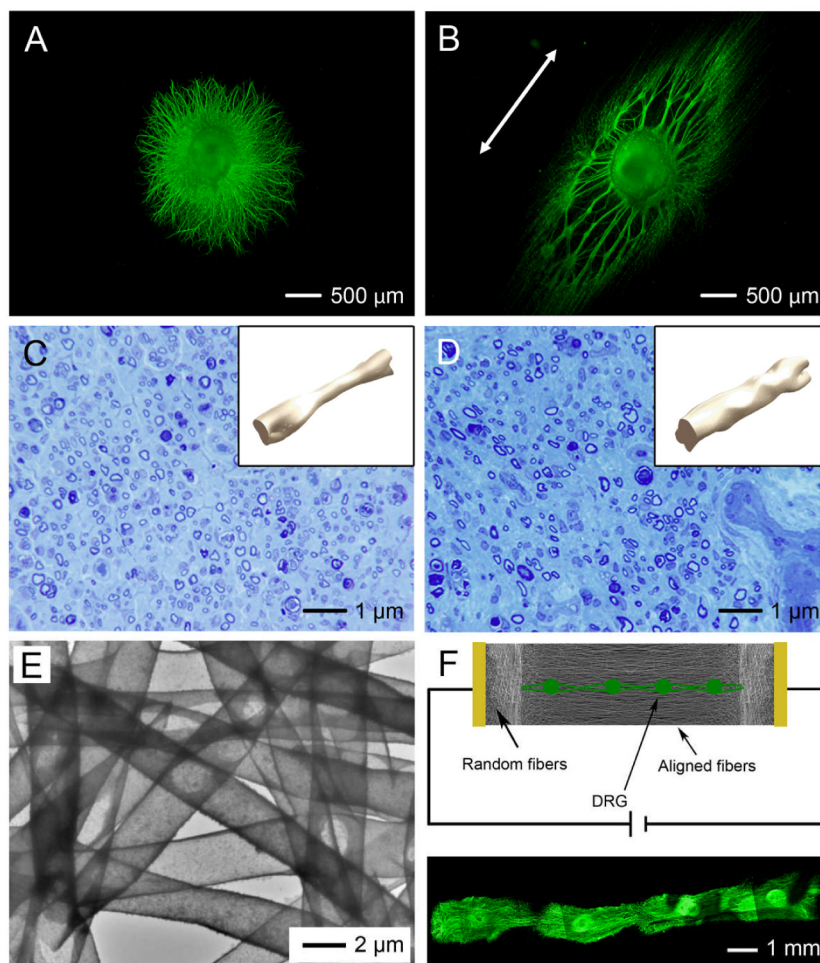
Figure 5.
Scaffolds of electrospun nanofibers for neural tissue engineering. A, B) Chicken dorsal root ganglia (DRG) cultured on scaffolds consisting of (A) random and (B) aligned nanofibers. Fiber alignment (as marked by the double-headed arrow) induced significantly longer extension of neurites from the DRG. C, D) Optical micrographs showing Toluidine Blue staining of a cross section at the midpoint of the nerve regenerated from distal parts through the guidance of (C) a silicone tube and (D) a conduit made of poly(3-caprolactone) nanofibers. The insets show isometric views of the regenerated nerves inside the silicone tube and the nanofiber-based conduit, respectively. E) Hollow nanofibers of polypyrrole (PPy) fabricated by dissolving the original PCL fibers after PPy coating. F) Electrical stimulation on multiple DRG cultured on a scaffold of aligned hollow PPy nanofibers led to the extension and potential connection of neurites from different DRG. Reproduced with permission: (A, B) from ref. [81], copyright2010 American Chemical Society; (C, D) from Ref. [85], copyright 2010 RSC Publishing; and (E, F) from Ref. [95], copyright 2009 Wiley-VCH.
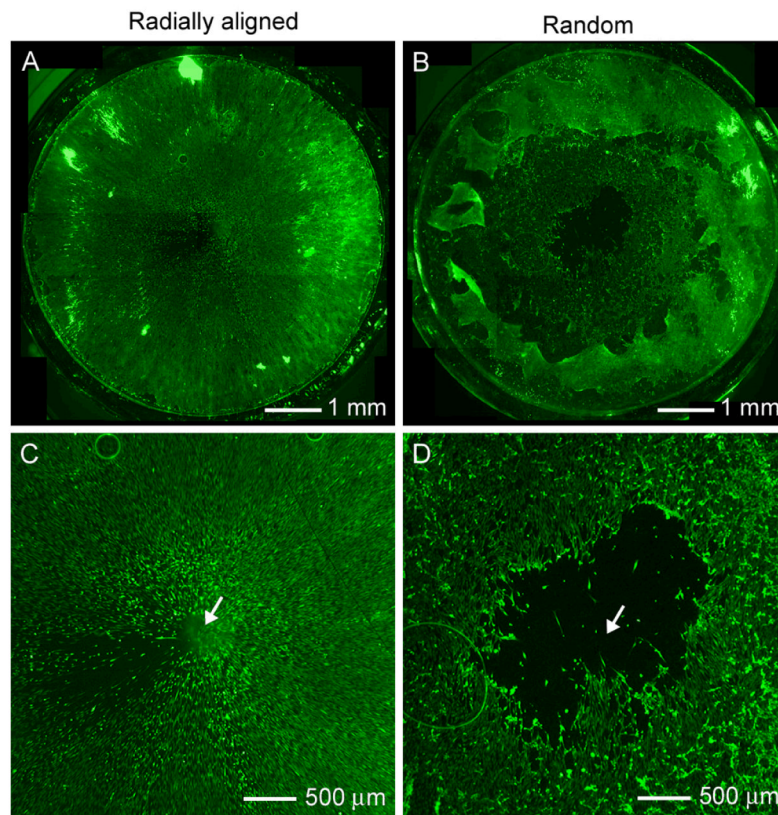
Figure 6.
Scaffolds of radially aligned nanofibers for dura mater repair. A, B) Fluorescence micrographs showing the migration of dura fibroblasts on scaffolds made of (A) radially aligned nanofibers and (B) random nanofibers, 7 days post seeding of the cells at the peripheries of the scaffolds. Radial alignment induced almost complete coverage of the scaffold by the cells, even at the center while there was a large void left in the center for the random nanofibers. C, D) Enlarged view of the center in (A) and (B), respectively. A clear void can be seen at the center for random nanofibers. Reproduced with permission: from Ref. [69], copyright 2010 American Chemical Society.
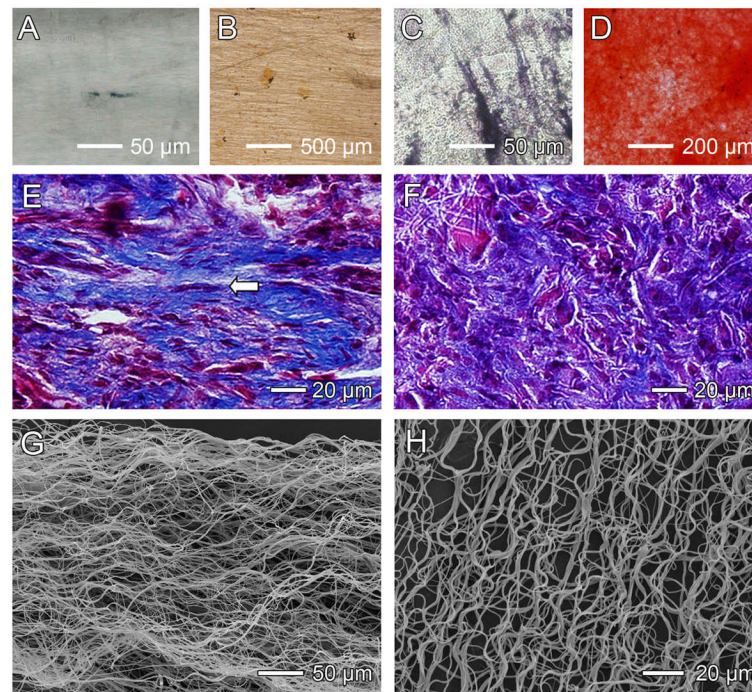
Figure 7.
Scaffolds of electrospun nanofibers for tendon/ligament repair. A–D) *In vitro* experiments showing osteogenesis, which was inhibited by the use of scaffolds with aligned fibers (A, B) as compared with scaffolds with random fibers (C, D). Osteogenesis was indicated by alkaline phosphatase (ALP) staining in black (A, C) and the mineral was marked by alizarin red staining in red (B, D). E, F) Masson's trichrome staining showing bands of collagen fibers formed when scaffolds of (E) aligned and (F) random nanofibers were used *in vivo* at week 6. Aligned fibers induced the formation of aligned collagen fibers (indicated by the arrow) similar to the native collagen fibrils. G) SEM image showing a scaffold of aligned but crimped nanofibers collected with a mandrel at a very high rotating speed. H) The crimped structure could be preserved even after 4-week immersion in phosphate-buffered saline (PBS). Reproduced with permission: (A–F) from Ref. [18], copyright 2010 Elseviser; and (G, H) from Ref. [106], copyright 2010 American Chemical Society.
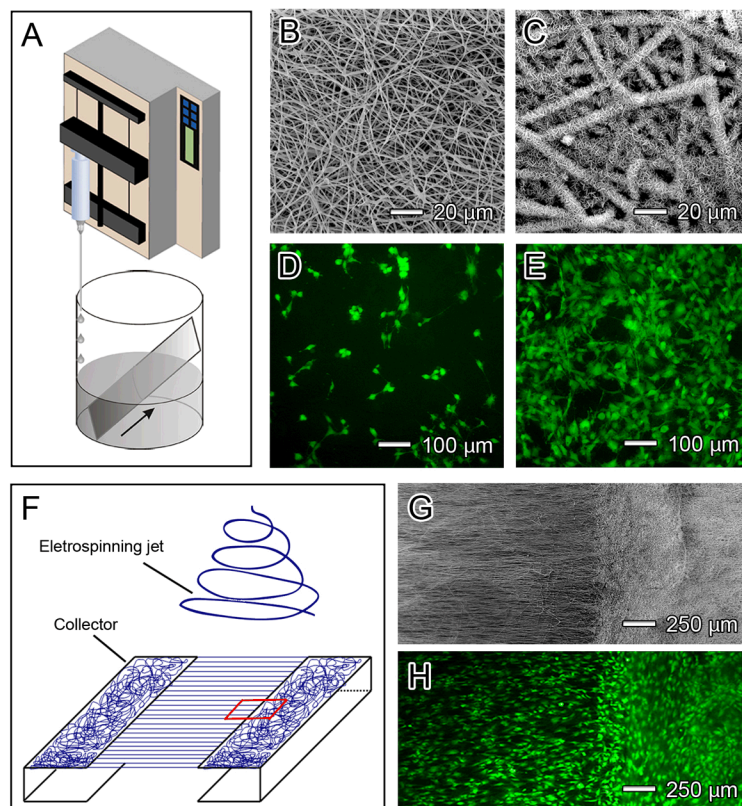
Figure 8.
Scaffold of electrospun nanofibers for tendon-to-bone insertion site repair. A) Schematic for generating a scaffold with a gradient in mineral coating. B, C) SEM images taken from two regions of the scaffold (B) low and (C) high in mineralization. D, E) Fluorescence micrographs showing MC3T3 preosteoblats attached to the two regions (D) low and (E) high in mineralization. F) Schematic for fabricating a scaffold with aligned-to-random transition for the nanofibers. G) SEM image showing the boundary between aligned and random fibers. H) Fluorescence micrograph showing morphologies of tendon fibroblasts seeded on the aligned and random sides of the scaffold. Reproduced with permission: (A–E) from Ref. [111b], copyright 2009 American Chemical Society; and (F–H) from Ref. [113a], copyright 2010 RSC Publishing.